POLITECNICO DI TORINO
Repository ISTITUZIONALE

Seismic in-plane displacement capacity of masonry barrel vaults: the role of constructive aspects

Original
Seismic in-plane displacement capacity of masonry barrel vaults: the role of constructive aspects / Alforno, M., Venuti, F., Monaco, A., Calderini, C.. - In: PROCEDIA STRUCTURAL INTEGRITY. - ISSN 2452-3216. - ELETTRONICO. - 44:(2023), pp. 1268-1275. (XIX ANIDIS Conference, Seismic Engineering in Italy Torino (Italy) 11-15 September 2022) [10.1016/j.prostr.2023.01.163].

Availability:
This version is available at: 11583/2976500 since: 2023-06-02T14:16:44Z

Publisher:
Elsevier

Published
DOI:10.1016/j.prostr.2023.01.163

Terms of use:

This article is made available under terms and conditions as specified in the corresponding bibliographic description in the repository

Publisher copyright

(Article begins on next page)

14 September 2026

Available online at www.sciencedirect.com

ScienceDirect

Procedia Structural Integrity 44 (2023) 1268–1275

Structural Integrity Procedia

www.elsevier.com/locate/procedia

XIX ANIDIS Conference, Seismic Engineering in Italy

Seismic in-plane displacement capacity of masonry barrel vaults: the role of constructive aspects

Marco Alforno[a]*, Fiammetta Venuti[a], Alessia Monaco[a], Chiara Calderini[b]

[a]*Politecnico di Torino, Viale Mattioli, 39, 10125, Torino, Italy*
[b]*Università di Genova, Via Montallegro 1, 16145, Genova, Italy*

Abstract

Historic masonry vaults are one of the most vulnerable elements with respect to the seismic action. Cracks are often detected after post-earthquake surveys. However, it is difficult to directly link the observed damage to causes. Different mechanisms can occur during an earthquake, such as in-plane horizontal shear distortion or longitudinal opening/closing of the abutments. These mechanisms are not necessarily associated to a specific crack pattern, since other factors are involved in the determination of the detected crack status. Among these factors, constructive aspects (such as the brick pattern) play a major role. This study aims at investigating the possible correlation between constructive aspects and the crack pattern in barrel vaults subjected to in-plane shear mechanism. Numerical simulations are carried out on an ideal circular vault with a rectangular base of dimensions 3.1x5.3 m, and rise of 1.175 m. Three brick patterns are considered: radial, diagonal and vertical. In order to investigate these aspects, a micro-modelling numerical approach has been adopted. Results are presented in terms of ultimate displacement capacity, collapse mechanisms and crack pattern charts.

© 2023 The Authors. Published by Elsevier B.V.
This is an open access article under the CC BY-NC-ND license (https://creativecommons.org/licenses/by-nc-nd/4.0)
Peer-review under responsibility of the scientific committee of the XIX ANIDIS Conference, Seismic Engineering in Italy.

Keywords: masonry; barrel vaults; brick pattern; shear mechanism

* Corresponding author.
E-mail address: marco.alforno@polito.it

2452-3216 © 2023 The Authors. Published by ELSEVIER B.V.
This is an open access article under the CC BY-NC-ND license (https://creativecommons.org/licenses/by-nc-nd/4.0)
Peer-review under responsibility of the scientific committee of the XIX ANIDIS Conference, Seismic Engineering in Italy.
10.1016/j.prostr.2023.01.163

1. Introduction

Historical masonry buildings are often characterized by the presence of vaulted structures, which represent some of the most vulnerable elements of traditional architecture with respect to the seismic action (Gaetani et al. 2016, Carfagnini et al. 2018, Bertolesi et al. 2019).

Cracks are often detected after post-earthquake surveys: however, it is difficult to directly link the observed damage to causes. Different mechanisms can occur during an earthquake, such as in-plane horizontal shear distortion or longitudinal opening/closing of the abutments (Rossi et al. 2016). These mechanisms are not necessarily associated to a specific crack pattern, since other factors are involved in the determination of the detected crack status. Among these factors, constructive aspects, such as the brick pattern, play a major role.

Vaults can be built according to different brick patterns. In historical building practices, they were generally chosen for technical reasons, e.g., the possibility to build without formwork (Wendland 2007). Barrel vaults were traditionally built according to four main patterns (Alforno et al. 2020, Lassaulx 1829; Breymann 1849; Choisy 1883, Gelati 1907): radial, with bed joint parallel to the abutments (Fig. 1a); vertical or pitched, with bed joints parallel to head arches (Fig. 1b); diagonal, with bed joint or head joints pointing towards the center of the vault (Fig. 1c); herringbone (Fig. 1d).

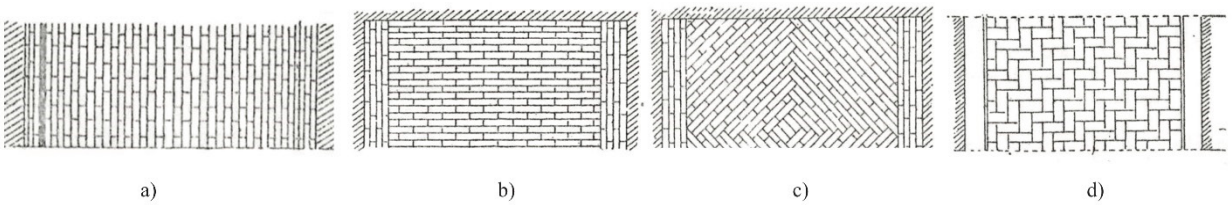

Fig. 1. Different types of brick patterns in barrel vaults (Gelati 1907): a) radial; b) vertical; c) diagonal, d) herringbone.

In the present work, barrel vaults of ideal geometry are modelled through the simplified micro-modelling approach in the framework of Finite Element Method (FEM) (Lourenço et al. 1995). This modelling approach has already been used by the authors (Alforno et al. 2020, Alforno et al. 2021a, Alforno et al. 2022) and successfully validated with physical in-scale models (Alforno et al. 2021b). The use of micro-mechanical models allows to simulate block-to-block interactions and therefore the real interlocking of bricks. In this work, three different brick arrangements are considered, i.e., radial, diagonal and vertical brick pattern. Static non-linear analyses are performed by applying a horizontal settlement of one of the abutments according to an in-plane shear mechanism until collapse. Results are analyzed in terms of capacity, ductility and collapse mechanism.

2. Description of the case study

2.1. Geometry and mechanical parameters

The chosen case study is a barrel vault with a rectangular base: the net span of the arch is approximately 3.1 m, the rise is about 1.175 m, and the length of the vault is 5.30 m. Three patterns were modeled: radial (R), diagonal (D) and vertical (V) (Fig. 2). The discretization of the vault's geometry was performed with blocks of the size of typical bricks (6 x 12 x 24 cm). All the geometrical models have been generated with the modelling software Rhinoceros and subsequently imported in Abaqus (2019) for the generation of the structural models.

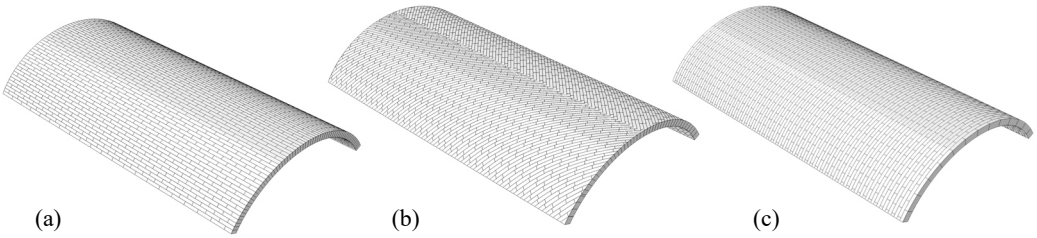

Fig. 2. Discretization of the barrel vault model with three patterns: a) radial; b) diagonal; c) vertical.

The discretization of the vaults' volume is performed through a simplified micro-modelling approach (Lourenço et al. 1995). This method has already been adopted and validated by the authors in previous papers (Alforno et al. 2020, Alforno et al. 2021a,b), where a detailed description of the adopted numerical approach is provided. In the present model, the mortar thickness is included within the dimension of the masonry blocks and the mechanical parameters adopted for both blocks and interfaces are set to take into account the role of the mortar joints. Interfaces are assumed as rigid in compression, by the introduction of a high value of normal stiffness k_n. The tensile strength of interfaces is null, whereas the definition of the tangential behavior is implemented through a purely frictional model, in which the contribution of cohesion is neglected and the static friction coefficient μ equals 0.5. The mechanical parameters adopted in the model are reported in Table 1. The adopted values are those suggested in Rossi et al. (2016) for historic brick masonry.

Table 1. Mechanical properties of blocks and interfaces.

Blocks			Interfaces	
ρ [kg/m^3]	E [MPa]	v [-]	μ [-]	k_n [N/m^3]
1800	1200	0.2	0.5	$5 \cdot 10^9$

The finite elements used for the bricks are linear hexahedra of 30 mm size, resulting in a maximum brick to element size ratio equal to 0.5. The blocks along the seam in the ridge of the diagonal barrel vault are modelled using second-order tetrahedra of the same approximate size. For the hexahedral elements the meshing technique is of structured type, while for the tetrahedra a free meshing algorithm has been adopted.

2.2. Load and boundary conditions

The vault is subject to its self-weight and to a horizontal settlement of one abutment in x direction, resulting in a shear mechanism (Fig. 3).

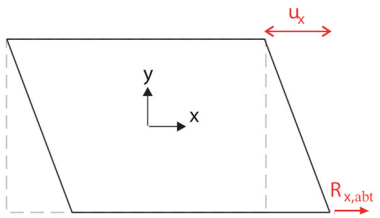

Fig. 3. Scheme of the imposed settlement and measured reaction forces at the abutments

The vaults are provided with confinement of the head arches, since the vault with diagonal pattern is not stable without lateral confinement. Actually, the not confined diagonal vault undergoes to local collapses of the head arches even under self-weight (Fig. 4). This is due to the fact that the diagonal brick courses exert a horizontal thrust against the head arches, which needs to be contrasted (Alforno et al. 2020). Confinement of the head arches is obtained through deformable boundary arches (DA), with about twice the vault thickness (27 cm) and 50 cm depth (Fig 5). DA are modelled with blocks with the same mechanical properties as the vault. Contact between the blocks of head arches and boundary structures is defined using the same interface behaviour adopted in the block-to-block contact definition. This means that normal compressive forces can arise, while no tension forces can develop. Shear forces along the planes of the boundary structures can be generated, depending on the normal forces, according to a Mohr-Coulomb criterion. Boundary conditions are applied to the blocks along the spring lines of the vault and to the supports of the Deformable Arches: all the nodes of the base surfaces are pinned.

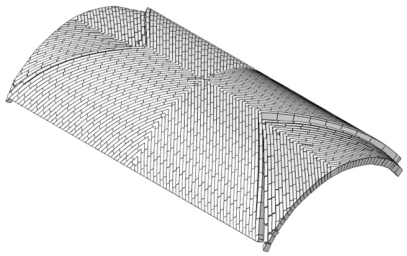

Fig. 4 Local collapse of the diagonal vault without lateral confinement

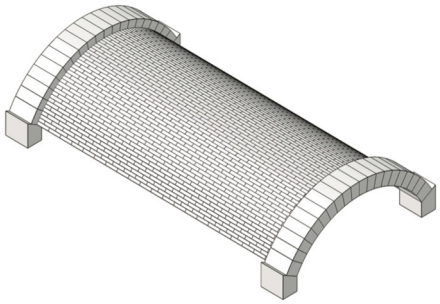

Fig. 5 Boundary deformable arches (DA)

2.3. Numerical analyses

Numerical simulations are carried out by adopting dynamic implicit analysis to investigate the structural behaviour under quasi-static regime, in order to control and stabilize the numerical convergence of the solution. Geometrical nonlinearities are taken into account. Each analysis is divided in two steps: first the structure is subjected to self-weight, then the settlement of the abutment is applied.

3. Results

Fig. 6 plots the resultant reaction forces $R_{x,tot}$ (sum of the reactions at the vault's moving abutments and on the deformable arches abutments), in the direction of the imposed displacement versus u_x. The reaction forces are normalized to the vault weight W (without considering the deformable arches' weight), while u_x is scaled with respect to the vault span L. The markers on the load displacement curves are referred to the value of imposed displacement

that corresponds to the activation of a failure mechanism. They have been identified by referring to the sudden increase in the differential vertical displacement of two bricks, highlighted in each vault in Fig 9.

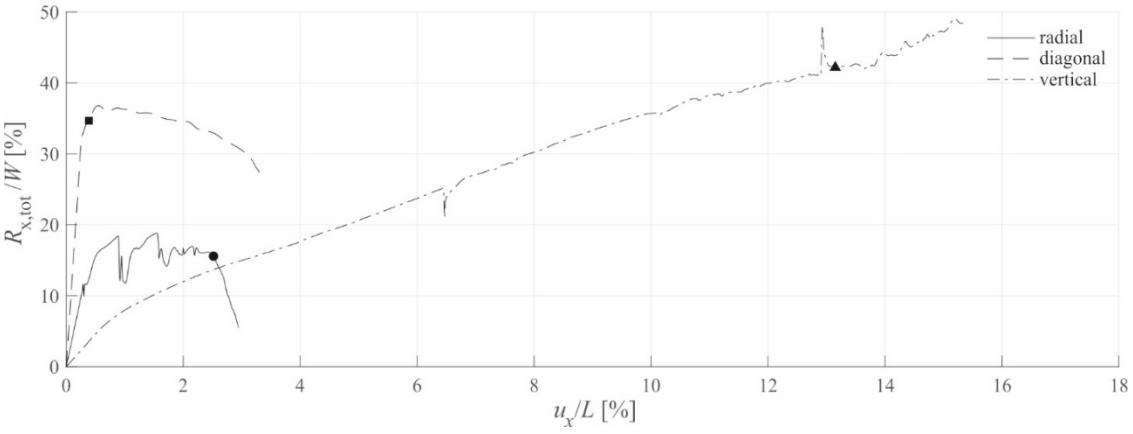

Fig. 6. Reaction forces $R_{x,tot}$ at the moving abutment and at the Deformable Arches versus imposed displacement

In order to compare the obtained load-displacement curves of total reaction force, the following quantities have been identified (Fig 7):

- R_{max}, corresponding to the peak value of the reaction force;
- u_{max}, corresponding to the maximum imposed settlement, i.e., the last point in the load-displacement curve;
- K_{el}, the elastic stiffness, calculated as the ratio R_{60}/u_{60} between the 60% of R_{max} and the corresponding settlement;
- the ductility u_{80}/u_{60}, where u_{80} is the settlement corresponding to R_{80}, i.e., to a post-peak 20% reduction of R_{max}. Note that u_{80} is assumed equal to u_{max} in case the reduction of R_{max} in the post-peak branch was less than 20%.

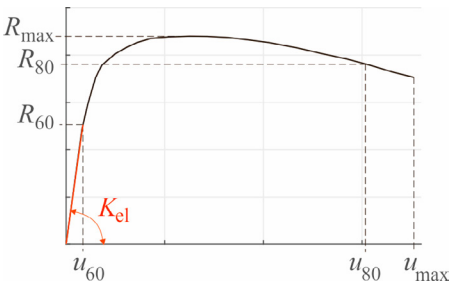

Fig. 7. Critical quantities monitored on the load-displacement curves

Table 3 reports the values of the above-defined quantities, while Table 4 reports their variation with respect to the radial pattern case, where $\Delta Q = (Q_{pattern}-Q_{radial})/Q_{radial} * 100$ and Q is the generic quantity.

Table 3. Table of critical quantities.

Pattern	R_{max} [N]	u_{max} [m]	K_{el} [N/m]	u_{80}/u_{60} [-]	u_{max} local [m]
Radial	7025	0.098	481714	9.03	0.077
Diagonal	14917	0.104	1415063	15.49	0.015
Vertical	19660	0.47	49376	1.97	0.407

Table 4. Percentage variation of peak reaction force, elastic stiffness and ductility with respect to the radial vault.

Pattern	ΔR_{max} [%]	ΔK_{el} [%]	$\Delta u_{80} / u_{60}$ [%]	Δu_{max} local [%]
Diagonal	71.61	193.76	171.61	-80.73
Vertical	-78.21	-89.75	21.79	425.89

On the basis of the above-defined quantities, the behaviour of the three vaults is quite different in terms of capacity, elastic stiffness and ductility. Specifically, the vertical vault is the one characterized by the lowest elastic stiffness (almost 90% lower than the radial vault) whereas the diagonal vault provides the greatest elastic stiffness, 193% greater than the radial vault. Local collapse occurs for small values of imposed displacement u_x in the diagonal vault (1.5 cm): this stage almost corresponds to the peak force value (R_{max}) of the system. In vertical and radial vaults, the local collapse happens at a more advanced stage of the analysis, toward the end of the load-displacement curves.

The deformed shapes at the end of the load displacement curves in Fig. 8 testify the influence of the masonry pattern on the collapse mechanism. Note that deformed shapes are plotted without boundary arches, with the exception of plan views and axonometric views, to better highlight the collapse mechanism of the vaults. In the radial vault, this involves the formation of hinges parallel to the x axis. When bricks are laid diagonally, a local failure starts at the crown of the vault, and it involves a few courses that point toward the center of the vault. In the vertical vault, cracks occur parallel to the bed joints (hence perpendicular to the x-axis), because separation of subsequent independent arches occur near the heads of the vault. The different deformation mechanism induced by different brick laying is also highlighted looking at the distribution of vertical displacements for fixed shear settlement of 0.33% (Fig. 9), which corresponds to the maximum displacement achieved by the diagonal vault before a local collapse at the crown is initiated. The maximum vertical displacements occur at the center of the vaults in the case of diagonal pattern, whereas in the other two cases deformations are localized at the head arches. In the case of the radial vault, the areas where maximum deformation occurs will correspond to the formation of longitudinal cracks. The vertical vault appears to be the less deformed at this stage of the test.

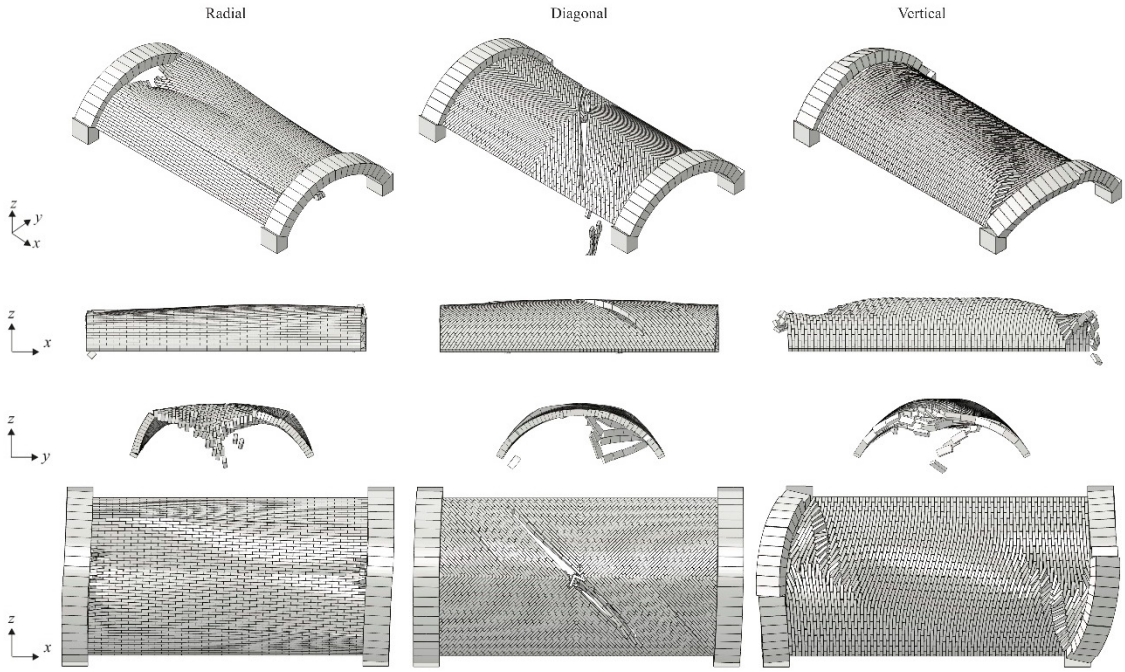

Fig. 8. Deformed shapes: axonometric view (first row), x-z plane view (second row), x-y plane view (third row) and plan view (fourth row).

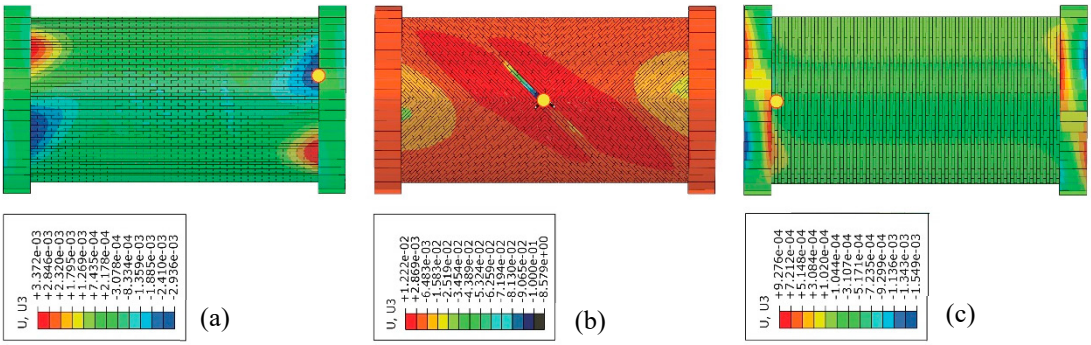

Fig. 9. Contour plot of u_z displacement [m] corresponding to an imposed vertical settlement u_z/L= 0.33 % for radial (a), diagonal (b) and vertical (c) pattern

The great capacity that the vertical vault shows, if compared to the other two vaults, may be the result of an overestimation due to some simplifications of the adopted mechanical model. As a matter of fact, the adopted constitutive law for blocks is linear elastic (infinite compressive strength) and the interaction law between blocks is rigid in compression. This may result in an overestimation of the strength of the assemblage with regard to stresses normal to bed joints. When the vertical pattern is used, bed joints are normal to the direction of the applied movement (x-axis), hence the role of normal stresses may be relevant in this assemblage, for the considered load case.

Finally, the chart in Fig. 10 summarizes the crack patterns associated to different brick laying. Longitudinal cracks develop in radial vaults, which follow the direction of the bed joints. In diagonal vaults the cracks also follow the bed joints, therefore they are inclined at a 45° angle. On the contrary, in vertical vaults cracks develop independently from the position of bed joints. A longitudinal crack is shown at the crown of the vault, but unlike radial vaults, this crack is visible from the extrados (hence, the hinge is located at the intrados). The information contained in this chart, along with the knowledge about the distribution of reaction forces in vaults built with different brick patterns, can inform the design of proper intervention techniques and methodologies.

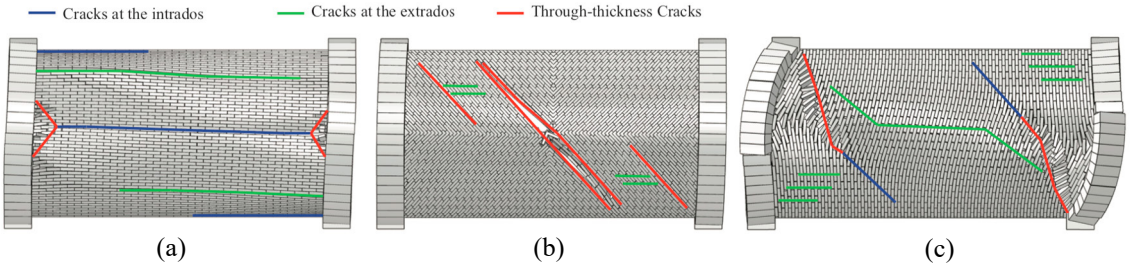

Fig. 10. Chart of the registered crack patterns for radial (a), diagonal (b) and vertical (c) brick patterns

4. Conclusions

This study has explored the role of some constructive aspects (brick pattern) on the shear in-plane capacity of masonry barrel vaults. Results of the numerical simulations have highlighted that the brick pattern greatly influences the structural behaviour of vaults subjected to horizontal settlement of the abutments in terms of ultimate capacity, ductility and collapse mechanism. Specifically, the vertical vault is the one characterized by the lowest elastic stiffness and peak force value, but by the greatest displacement capacity. Conversely, the diagonal vault provides the greatest elastic stiffness, but the lowest displacement capacity.

Moreover, a crack pattern chart is provided for each brick pattern, in order to help practitioners to correctly identify possible causes and design proper interventions.

References

Abaqus Theory Manual. 2019. Dassault Systemes.

Alforno, M., Venuti, F., Monaco, A. and Calderini, C., 2022. Seismic behaviour of cross vaults with different brick pattern. Bulletin of Earthquake Engineering, https://doi.org/10.1007/s10518-022-01347-6.

Alforno, M., Venuti, F., Monaco, A. and Calderini, C., 2021a. Numerical investigation of the influence of constructive aspects on the structural behaviour of masonry cross vaults. International Journal of Architectural Heritage, DOI: 10.1080/15583058.2021.1992534.

Alforno, M., Monaco, A., Venuti, F., Calderini, C., 2021b. Validation of simplified micro-models for the static analysis of masonry arches and vaults. International Journal of Architectural Heritage 15, 1196-1212.

Alforno, M., Venuti, F., Monaco, A., 2020. The structural effects of micro-geometry on masonry vaults. Nexus Network Journal 22, 1237–1258.

Bertolesi, E., Adam, J.M., Rinaudo, P., Calderon, P.A., 2019. Research and practice on masonry cross vaults: a review. Engineering Structures 180, 67–88.

Breymann, G. A., 1849. Allgemeine Bau-Constructions-Lehre, mit besonderer Beziehung auf das Hochbauwesen. Vol. 1: Constructionen in Stein. Hoffmann, Stuttgart.

Carfagnini C., Baraccani S., Silvestri S., Theodossopoulos D., 2018. The effects of in-plane shear displacements at the springings of Gothic cross vaults. Construction and Building Materials 186, 219–232.

Choisy A., 1883. L'art de batir chez les Byzantines, Société anonyme de publications périodiques, Paris.

Gaetani, A., Monti, G., Lourenco, P.B., Marcari, G., 2016. Design and analysis of cross vaults along history. International Journal of Architectural Heritage 10, 841–856.Lourenco, P.B., Rots, J.G., Blaauwendraad, J., 1995.Two approaches for the analysis of masonry structures - micro and macro-modeling. HERON 40:4, 313-340.Gelati, C. 1907. Nozioni pratiche ed artistiche di architettura. 2nd ed. (1st edition, 1899). Torino: Carlo Pasta.

Rossi, M., Calderini, C., Lagomarsino, S., 2016. Experimental testing of the seismic in-plane displacement capacity of masonry cross vaults through a scale model. Bulletin of Earthquake Engineering 14, 261-281.

Wendland, D., 2007. Traditional vault construction without formwork: masonry pattern and vault shape in the historical technical literature and in experimental studies. International Journal of Architectural Heritage 1:4, 311-365.

Lassaulx, J.C., 1829. Beschreibung des Verfahrens bei Anfertigungleichter Gewolbeuber Kirchen und ahnlichen Raumen, Journal fur die Baukunst 1:4, 317-330.